Kalman Filtering with Harmonics Whitening for P Class Phasor Measurement Units

Amir Bashian, David Macii, Daniele Fontanelli and Dario Petri
Department of Industrial Engineering
University of Trento
Trento, Italy
david.macii@unitn.it

***Abstract*—The need for increasingly accurate and fast Phasor Measurement Units (PMUs), especially for active distribution systems monitoring, requires to achieve challenging trade-offs between measurement uncertainty and responsiveness. This is particularly important for protection-oriented (i.e., *P Class*) PMUs. In order to improve estimation accuracy with no need to prolong the data record size and the related delays, this paper presents a Taylor Kalman Filter (TKF) enhanced with a preliminary stage able to whiten possible narrowband disturbances over short observation intervals. The use of dynamic estimators such as the TKF is motivated by the need to track possible sudden amplitude or phase changes of voltage or current AC waveforms, which are likely to occur in smart grids. However, while a basic TKF is very sensitive to disturbances different from white noise, the proposed whitening-technique is able to greatly improve the estimation accuracy of synchrophasor amplitude, phase, frequency and Rate of Change of Frequency (ROCOF) under the influence of harmonics and amplitude or phase step changes even over one-cycle observation intervals, with just a minor performance degradation in the other *P Class* testing conditions reported in the IEEE/IEC Standard 60255-118-1:2018.**

Keywords—phasor measurement units (PMU), whitening, phasor estimation, Kalman Filter, smart grids, power system measurements and monitoring.

I. INTRODUCTION

The growing penetration of distributed generators (DGs) and power electronic devices at the distribution level leads to new challenges in low-voltage and medium-voltage networks [1]. Demand side fluctuations, supply side volatility, network harmonics and inter-harmonics can affect the proper operation and control of smart grids [2]-[3]. To detect and counteract possible critical operating conditions, the state of the system should be estimated also at the distribution level [4]–[6]. The Phasor Measurement Units (PMUs) are particularly useful to this purpose, since they are able to estimate the synchronized phasors of voltage and current AC waveforms at a high rate under both static and dynamic conditions. Unfortunately, the measurement of amplitude, phase angle, frequency, and the rate of change of frequency (ROCOF) is affected by a variety of uncertainty contributions, that are particularly critical for distribution systems monitoring. For this reason, several estimation algorithms for PMUs have been recently proposed in the scientific literature [7].

The IEEE/IEC Standard 60255-118-1-2018 (briefly referred to as “the IEEE/IEC Standard” in the rest of this paper) specifies two classes of PMUs depending on the intended applications type [8]. For high-accuracy measurement purposes, the so-called *M Class* is required. However, for protection purposes lower accuracy is acceptable provided that shorter response times are achieved. For this kind of applications, the so-called *P Class* specifications are defined in the Standard. Either PMU class must comply with its own set of performance limits expressed in terms of *Total Vector Errors* (TVE), *Frequency Err*ors (FE), *Rate of change of Frequency Errors* (RFE) and, in the case of amplitude or phase step changes, also response times and delay times. Although these limits were established mainly on the basis of the requirements of transmission systems, they are currently adopted also as a reference for distribution-level PMUs. However, because of the characteristics of distribution systems (e.g., smaller angle differences between bus voltage phasors, lower *X/R* ratios than in transmission networks and larger harmonics and inter-harmonics relative amplitude [9]), new, faster and increasingly accurate algorithms are needed. The estimation algorithms for PMUs are divided generally into two broad categories: the frequency-domain and the time-domain techniques [10].

The frequency-domain techniques are generally based on the Discrete Fourier Transform (DFT). Generally, they ensure good performances with a low computational burden especially in steady-state conditions provided that the effect of possible off-nominal frequency deviations is estimated and compensated and that observation intervals of suitable length are considered [11]. However, their performance degrades when dynamic disturbances (e.g., oscillations) affect the power systems AC waveforms [12]. One of the most famous examples of this kind of algorithms is the interpolated DFT (IpDFT) [13].

To achieve better results under dynamic operating conditions, a variety of time-domain algorithms based on the Taylor’s series expansion of the function modeling the synchrophasor time-varying behavior were proposed [14]. One of the best known methods of this type is the Taylor Weighted Least Squares (WLS) estimator, also called Taylor-Fourier Filter [15], which is indeed particularly accurate under dynamic testing conditions. However, if static off-nominal frequency deviations occur, the accuracy of this approach decreases, unless such frequency deviations are estimated and its effect is compensated [16]. Also, when low-order harmonics or inter-harmonics affect the AC waveform, the effectiveness of this method is reduced. Relevant improvements can be obtained by estimating and compensating for the effect of a given number of harmonics (e.g., through the Taylor-Fourier Transform or a multi-step corrected IpDFT [17]-[18]) and, if possible, by extending a similar approach to the case of inter-harmonics (e.g., through compressive sensing [19], or the iterative IpDTF presented in [20]). However, the additional computational burden due to multi-tone estimation and compensation can be noticeable. This problem becomes critical when real-time processing and high-rate reporting rates are required, especially for *P Class* PMUs. Therefore, an algorithm able to improve accuracy under the effect of narrowband disturbances even over short observation intervals would be very useful.

In this respect, this paper addresses this problem through a preliminary whitening of possible narrowband disturbances (especially harmonics) prior to estimating the parameters of an AC waveform. This idea is not totally new, as it was firstly introduced in [21], where it was applied and tested by using the classic TWLS estimator as a benchmark [15]. In this paper, a similar approach is applied to a Kalman Filter based on the Taylor's series expansion of the function modeling the synchrophasor evolution over time. In the following, this estimator will be denoted simply as TKF for brevity. The rationale for this choice is that Kalman filters are natively conceived to track possible changes of the state variables to be estimated. In fact, various KFs for PMUs have been already suggested in the literature [22]–[25]. However, KFs are notoriously sensitive to narrowband disturbances and they could greatly benefit of a technique for disturbance whitening. This is true especially when short observation intervals are considered, since the impact of such disturbances is higher than over intervals consisting of several power line cycles.

The rest of the paper is structured as follows. In Section II, the proposed Whitening-based Taylor Kalman Filter (W-TKF) method is described. In Section III, the simulation results obtained with the W-TKF estimator are presented and compared with those of a basic TKF to show the effectiveness of the proposed methodology. Finally, in Section IV, the main conclusions are summarized.

II. Estimator Description

A generic AC voltage or current waveform acquired by a PMU can be modelled as follows

$$s(t) = x(t)+d(t)+\varepsilon(t) = a(t)\cos[2\pi f\, t + \varphi(t)]+d(t)+\varepsilon(t), \quad (1)$$

where

- $a(t)$ and $\varphi(t)$ are the time-varying amplitude and phase of the ideal AC waveform $x(t)$, respectively;
- $f = f_0 + \delta$ is the fundamental power system frequency, which may differ from the nominal value $f_0 = 50$ Hz or 60 Hz by a fraction δ, e.g., due to possible mismatches between power demand and supply;
- $d(t)$ represents the sum of the most significant steady-state harmonic or inter-harmonic disturbances and finally
- $\varepsilon(t)$ is a white and normally distributed noise with zero-mean and variance σ_ε^2 affecting the input waveform before PMU acquisition.

Observe that both $a(t)$ and $\varphi(t)$ are regarded as functions of time, as they need to be measured and tracked in real-time if the operating conditions of the grid are not stationary.

Of course, the synchrophasor $p(t_r) = \frac{a(t_r)}{\sqrt{2}} e^{j\varphi(t_r)}$, the instant frequency $f(t_r) = f + \frac{1}{2\pi}\left.\frac{d\varphi(t)}{dt}\right|_{t_r}$ and the ROCOF $\frac{d\,f(t_r)}{dt} = \frac{1}{2\pi}\left.\frac{d^2\varphi(t)}{dt^2}\right|_{t_r}$ at the UTC reference time t_r depend on both the number of collected data and on the position of t_r within the observation interval considered. Assuming that

- $M = [f_s/f_0]$ (with f_s and $[\cdot]$ being the PMU sampling rate and the "rounding to the nearest integer" function, respectively) represents the integer number of samples per nominal cycle;
- C is the supposedly integer number of nominal cycles observed in each observation interval;
- t_r lies exactly in the center of this interval to minimize the error due to the truncation of the Taylor's series of the phasor [22];

then the size of the data record used for waveform parameter estimation is $N = M\cdot C$ and the sequence of collected samples is

$$s(n_r) = a(n_r)\cos\left[2\pi\frac{f}{f_s}n_r + \varphi(n_r)\right] + d(n_r) + \varepsilon'(n_r), \quad (2)$$

where (assuming without loss of generality that N is odd) $t_r\cdot f_s - \frac{N-1}{2} \le n_r \le t_r\cdot f_s + \frac{N-1}{2}$. Sequence (2) be rearranged as a single N-long column vector $\boldsymbol{s}_r$. Note that $\varepsilon'(n_r)$ is different from $\varepsilon(n_r)$ because it includes the additional wideband random contributions due to measurement transducer noise, front-end analog circuitry noise, quantization noise and, last but not least, sampling jitter and synchronization uncertainty. Therefore, its variance $\sigma_{\varepsilon'}^2$ is greater than σ_ε^2.

In the following subsections, first the whitening technique is recalled and then the TKF estimator is described.

A. Disturbance whitening

Let us assume that $d(t)$ in (1) and (2) consists of D significant narrowband harmonic or inter-harmonic components emerging from the noise floor. By applying the singular value decomposition to the correlation matrix of $\boldsymbol{s}_r$ it follows that [21]

$$Q_r = E\{\boldsymbol{s}_r \cdot \boldsymbol{s}_r^T\} = SLS^T = S\begin{bmatrix}\Lambda_0 & 0\\ 0 & \tilde{\Lambda}_0\end{bmatrix}S^T, \quad (3)$$

where S is an $N \times N$ orthogonal matrix whose columns are the eigenvectors of Q_r, Λ_0 is a 2×2 diagonal matrix including the eigenvalues associated with the fundamental component of (1) and

$$\tilde{\Lambda}_0 = \begin{bmatrix}\Lambda_D & 0\\ 0 & \sigma_{\varepsilon'}^2 I_{N-2\cdot(D+1)}\end{bmatrix} \quad (4)$$

is a $(N$-2$) \times (N$-2$)$ diagonal matrix comprising the eigenvalues associated with all the other disturbances, i.e., D pairs of eigenvalues (in matrix Λ_D) due to possible narrowband harmonic and inter-harmonic components and N-2$\cdot(D$+1$)$ identical eigenvalues $\sigma_{\varepsilon'}^2$ related to the noise vector subspace. Clearly, symbol I denotes the identity matrix, whose size is specified in the subscript.

As proved in [21], after identifying the eigenvalues in Λ_0 (which is quite simple since they are certainly the largest ones), harmonics and inter-harmonics whitening can be achieved by applying the following linear transformation to the raw data record $\boldsymbol{s}_r$, i.e.

$$\boldsymbol{y}_r = W\boldsymbol{s}_r, \quad (5)$$

where

$$W = S\begin{bmatrix}I_2 & 0\\ 0 & \sigma_{\varepsilon'}\tilde{\Lambda}_0^{-\frac{1}{2}}\end{bmatrix}S^{-1}. \quad (6)$$

If the eigenvalues of $\tilde{\Lambda}_0$ were known exactly, the correlation matrix $E\{\boldsymbol{y}_r\cdot\boldsymbol{y}_r^T\}$ would include only the eigenvalues associated with the fundamental component in Λ_0, while all the other N-2 eigenvalues would be equal to $\sigma_{\varepsilon'}^2$. However, in practice matrix Q_r can just be estimated from the available data record. Therefore, the uncertainty associated with Q_r estimation may partially degrade the effectiveness of disturbance whitening.

B. Taylor Kalman Filter (TKF)

As briefly explained in the Introduction, the TKF results from the Taylor's series expansion of the phasor $p(t)$ around the reference time t_r. In practice, the Taylor's series can be truncated to the second order since using higher-order coefficients does not lead to significant accuracy improvements [22], i.e.

$$p(n_r) = p_r(n) \approx p_{0,r}+p_{1,r}n+p_{2,r}n^2 \qquad (7)$$

where $-\frac{N-1}{2} \leq n \leq \frac{N-1}{2}$ and $p_k=\frac{1}{k!}\frac{1}{f_s^k}\frac{d^k p}{dt^k}\Big|_{t_r}$ for $k = 0,1,2$. Therefore, if disturbances $d(t)$ and $\varepsilon(t)$ are negligible, then $s(n_r) \approx x(n_r)$ and (2) can be expressed as a function of (7) as

$$x(n_r)\approx\frac{(p_{0,r}+p_{1,r}n+p_{2,r}n^2)e^{j2\pi\frac{f}{f_s}n}+(p_{0,r}^*+p_{1,r}^*n+p_{2,r}^*n^2)e^{-j2\pi\frac{f}{f_s}n}}{2} \qquad (8)$$

where * denotes the complex conjugate operator. Therefore, if the Taylor's series coefficients are included into a single column vector $\boldsymbol{p}_r=\left[p_{2,r},p_{1,r},p_{0,r},p_{0,r}^*,p_{1,r}^*,p_{2,r}^*\right]^{\mathrm{T}}$, assuming that the observation interval shifts by one sample at a time, it can be easily shown that the dynamic of the synchrophasor after one time step is given by [22]

$$\boldsymbol{p}_{r+1}=A\,\boldsymbol{p}_r \qquad (9)$$

where the system matrix is

$$A=\begin{bmatrix}1&0&0&0&0&0\\2&1&0&0&0&0\\1&1&1&0&0&0\\0&0&0&1&1&1\\0&0&0&0&1&2\\0&0&0&0&0&1\end{bmatrix}. \qquad (10)$$

Moreover, expression (8) can be rearranged into a matrix form as follows, i.e.

$$\boldsymbol{x}_r=B_r\,\boldsymbol{p}_r \qquad (11)$$

where $\boldsymbol{x}_r$ is the vector of ideal samples and $B_r = [B_{r,1}\ B_{r,2}]$ is a $N \times 6$ matrix that, if N is odd, consists of

$$B_{r,1}=\frac{1}{2}\begin{bmatrix}\left(-\frac{N-1}{2}\right)^2 e^{j\left(\frac{N-1}{2}\right)\left(\frac{2\pi}{M}\right)} & \left(-\frac{N-1}{2}\right)e^{j\left(\frac{N-1}{2}\right)\left(\frac{2\pi}{M}\right)} & e^{j\left(\frac{N-1}{2}\right)\left(\frac{2\pi}{M}\right)}\\ \vdots & \vdots & \vdots\\ 0 & 0 & 1\\ \vdots & \vdots & \vdots\\ \left(\frac{N-1}{2}\right)^2 e^{-j\left(\frac{N-1}{2}\right)\left(\frac{2\pi}{M}\right)} & \left(\frac{N-1}{2}\right)e^{-j\left(\frac{N-1}{2}\right)\left(\frac{2\pi}{M}\right)} & e^{-j\left(\frac{N-1}{2}\right)\left(\frac{2\pi}{M}\right)}\end{bmatrix},$$

and

$$B_{r,2}=\frac{1}{2}\begin{bmatrix}e^{-j\left(\frac{N-1}{2}\right)\left(\frac{2\pi}{M}\right)} & \left(-\frac{N-1}{2}\right)e^{-j\left(\frac{N-1}{2}\right)\left(\frac{2\pi}{M}\right)} & \left(-\frac{N-1}{2}\right)^2 e^{-j\left(\frac{N-1}{2}\right)\left(\frac{2\pi}{M}\right)}\\ \vdots & \vdots & \vdots\\ 1 & 0 & 0\\ \vdots & \vdots & \vdots\\ e^{j\left(\frac{N-1}{2}\right)\left(\frac{2\pi}{M}\right)} & \left(\frac{N-1}{2}\right)e^{j\left(\frac{N-1}{2}\right)\left(\frac{2\pi}{M}\right)} & \left(\frac{N-1}{2}\right)^2 e^{j\left(\frac{N-1}{2}\right)\left(\frac{2\pi}{M}\right)}\end{bmatrix}.$$

Note that the ideal data vector $\boldsymbol{x}_r$ in (11) can be replaced by

$$\boldsymbol{z}_r=\begin{cases}\Omega\,\boldsymbol{s}_r & \text{without disturbance whitening}\\ \Omega\,\boldsymbol{y}_r & \text{with disturbance whitening}\end{cases} \qquad (12)$$

where Ω is an $N \times N$ diagonal matrix whose diagonal elements are the coefficients of a possible window function (e.g., $\Omega = I$ if the rectangular window is used). Thus, the dynamic system that is used to build the TKF results from the combination of (9), (11) and (12), i.e.

$$\begin{cases}\boldsymbol{p}_{r+1}=A\boldsymbol{p}_r+\boldsymbol{\eta}_r\\ \boldsymbol{z}_r=H_r\boldsymbol{p}_r+\boldsymbol{w}_r\end{cases} \qquad (13)$$

where $\boldsymbol{\eta}_r$ is the column vector including the synchrophasor model errors (e.g., due to both Taylor's series truncation and possible components that are not included in the signal model), $H_r = \Omega B_r$ and $\boldsymbol{w}_r$ is the measurement noise vector either with or without disturbance whitening. Of course, the elements of $\boldsymbol{w}_r$ depend on $\varepsilon'(\cdot)$ within the r-th data record, namely for $t_r \cdot f_s - \frac{N-1}{2} \leq n_r \leq t_r \cdot f_s + \frac{N-1}{2}$, but they are supposed to be extracted from a stationary wideband random noise process.

From the Kalman filter definition applied to (13), it follows that in the *prediction step* [26]

$$\begin{cases}\hat{\boldsymbol{p}}_{r+1}^{+}=A\,\hat{\boldsymbol{p}}_r\\ \Gamma_{r+1}^{+}=A\Gamma_r A^T+E\end{cases} \qquad (14)$$

where superscript $^+$ and symbol $\hat{}$ represent the one-step predicted and estimated quantities, respectively, Γ_r is the state estimation covariance matrix and E is the covariance matrix of $\boldsymbol{\eta}_r$, which is supposed to be constant as the synchrophasor model errors can be regarded as extracted from a stationary wideband random noise process.

In the *update step* of the filter we have that

$$\begin{cases}\hat{\boldsymbol{p}}_{r+1}=\hat{\boldsymbol{p}}_{r+1}^{+}+G_{r+1}(\boldsymbol{z}_r - H_r\hat{\boldsymbol{p}}_{r+1}^{+})\\ \Gamma_{r+1}=(I_6 - G_{r+1}H_r)\Gamma_{r+1}^{+}\end{cases} \qquad (15)$$

where

$$G_{r+1}=\Gamma_{r+1}^{+}H_r^T\left(H_r\Gamma_{r+1}^{+}H_r^T+R\right)^{-1} \qquad (16)$$

is the so-called Kalman gain matrix and R in (16) is the covariance matrix associated with $\boldsymbol{w}_r$.

By using the elements of $\hat{\boldsymbol{p}}_r$, the frequency and ROCOF values can be finally estimated as follows [15]:

$$\hat{f}_r=f_0+\frac{f_s}{2\pi\left|\hat{p}_{0,r}\right|^2}Im\left\{\hat{p}_{1,r}\,\hat{p}_{0,r}^*\right\}, \qquad (17)$$

$$\widehat{ROCOF}_r=\frac{f_s^2}{\pi}\left[\frac{Im\{\hat{p}_{2,r}\hat{p}_{0,r}^*\}}{\left|\hat{p}_{0,r}\right|^2}-\frac{Re\{\hat{p}_{1,r}\hat{p}_{0,r}^*\}\,Im\{\hat{p}_{1,r}\hat{p}_{0,r}^*\}}{\left|\hat{p}_{0,r}\right|^4}\right], \qquad (18)$$

where functions $Re\{\cdot\}$ and $Im\{\cdot\}$ return the real and imaginary parts, respectively, of their argument.

III. Simulation Results

The accuracy of both the basic TKF and the W-TKF were evaluated through Monte Carlo simulations in the *P Class* testing conditions of the IEEE/IEC Standard 60255-118-1:2018 [8], i.e.

- setting an off-nominal frequency deviation δ within ±2 Hz;
- adding individual harmonics (from the 2nd to 50th) with amplitude equal to 1% of the fundamental and considering δ = ±2 Hz;
- including an Amplitude Modulation (AM) oscillation with a modulation index equal to 0.1 and frequency equal to 2 Hz;
- including a Phase Modulation (PM) oscillation of amplitude equal to 0.1 rad and frequency equal to 2 Hz;
- considering a ±10% amplitude step change;
- considering a ±π/18 phase step change;
- assuming that the system frequency changes linearly within ±2 Hz with respect to the fundamental frequency f_0 at a rate of ±1 Hz/s.

In all cases, the AC waveform nominal amplitude is 1 p.u., the nominal system frequency f_0 is 50 Hz and the initial phase angles are swept linearly within [-π, π]. The phase values of harmonics and modulating tones are changed randomly between [-π, π], with a uniform probability density function. Every test was repeated 100 times. The sampling frequency f_s is 5 kHz. The SNR used to determine the σ_{ε}^{2}, values is 64 dB. For TKF implementation, the state estimation covariance matrix Γ_0 is initialized with large diagonal dummy values (i.e., 10). The elements of covariance matrix E in (14) result from the worst-case truncation errors of the Taylor's series coefficients between reference times t_r and t_{r+1}, assuming that the phasor is affected by low-frequency amplitude and phase oscillations equal to 10% of the fundamental amplitude and 0.1 rad, respectively. As a result, the diagonal elements of E range from about 2×10^{-5} for $p_{2,r}$ and $p^{*}_{2,r}$ to 4×10^{-3} for $p_{0,r}$ and $p^{*}_{0,r}$, respectively. The elements of R depend instead on both the noise floor of the measurement system and the window functions chosen to weigh the samples within a given observation interval. Recalling that C denotes the number of nominal power line cycles within every observation interval, two types of window functions are adopted in this paper, i.e., the rectangular window and the Hann window over $C = 1$ cycle or $C = 2$ cycles intervals. With both windows, matrix R in (16) is diagonal. However, while the elements of R with the rectangular window are the same (in the order of about 4×10^{-7}), when the Hann window is used the diagonal elements of matrix R are shaped accordingly.

The correlation matrix Q_r in (3) is estimated over two subsequent N-long observation intervals as explained in [21].

Tables I and II show the maximum TVE, absolute FE, and absolute RFE values obtained with the basic TKF and the proposed W-TKF using the rectangular and the Hann window, respectively, by shifting the observation interval by one sample at a time. In the phase step tests, the peak |FE| and |RFE| resulting at the exact times when the ideal step occurs are excluded since the derivative of such perfect steps should be a Dirac pulse. Therefore, the corresponding |FE| and |RFE| values would tend to infinity, which is not realistic. Quite importantly, the reported step test results do not refer to the response times (as prescribed by the Standard), but again to the maximum TVE, |FE| and |RFE| values since the focus of this paper is just on estimation accuracy analysis.

TABLE I. MAXIMUM TVE, |FE| AND |RFE| VALUES OBTAINED WITH THE TKF AND W-TKF ESTIMATORS OVER ONE-CYCLE AND TWO-CYCLE INTERVALS USING THE RECTANGULAR WINDOW THE *CLASS P* LIMITS OF THE IEEE/IEC STANDARD 60255-118-1:2018 (WHEN SPECIFIED) ARE ALSO SHOWN.

Test Condition	TVE$_{aax}$ [%]					$\|FE\|_{max}$ [mHz]					$\|RFE\|_{max}$ [Hz/s]				
	Lim.	$C = 1$		$C = 2$		Lim.	$C = 1$		$C = 2$		Lim.	$C = 1$		$C = 2$	
		TKF	*W-TKF*	*TKF*	*W-TKF*		*TKF*	*W-TKF*	*TKF*	*W-TKF*		*TKF*	*W-TKF*	*TKF*	*W-TKF*
Freq. Dev. only (±2 Hz)	1	0.09	0.09	0.04	0.04	5	21	22	16	16	0.4	10.6	9.7	0.9	1.0
Freq. Dev (±2Hz) + 1% 2nd Harmonic	1	1.90	0.20	0.30	0.08	5	274	34	43	17	0.4	240	25.0	8.9	1.3
Freq. Dev (±2Hz) + 1% 3rd Harmonic	1	0.83	0.15	0.17	0.09	5	259	34	30	17	0.4	116	17.0	5.4	1.2
Freq. Dev (±2Hz) + 1% 50th Harmonic	1	0.20	0.09	0.05	0.04	5	44	23	18	16	0.4	25.0	9.5	1.1	0.9
AM (2 Hz 10% modulating tone)	3	0.10	0.11	0.04	0.09	60	16	15	3	5	2.3	9.8	9.0	0.7	0.8
PM (2 Hz 0.1 rad modulating tone)	3	0.08	0.10	0.04	0.08	60	13	22	4	48	2.3	9.0	10.0	0.7	1.0
Step Test (±10% amplitude change)	-	8.00	6.00	5.70	5.90	-	729	214	140	49	-	420	86.0	26.0	5.8
Step Test (±π/18 phase angle change)	-	14.60	10.50	9.70	10.30	-	2726	1372	1120	683	-	823	216	135	34.2
Linear freq. ramp (within ±2 Hz @±1 Hz/s)	1	0.09	0.09	0.04	0.06	10	18	19	14	30	0.4	10.8	9.7	0.9	1.0

TABLE II. MAXIMUM TVE, |FE| AND |RFE| VALUES OBTAINED WITH THE TKF AND W-TKF ESTIMATORS OVER ONE-CYCLE AND TWO-CYCLE INTERVALS USING THE HANN WINDOW. THE *CLASS P* LIMITS OF THE IEEE/IEC STANDARD 60255-118-1:2018 (WHEN SPECIFIED) ARE ALSO SHOWN.

Test Condition	TVE$_{aax}$ [%]					$\|FE\|_{max}$ [mHz]					$\|RFE\|_{max}$ [Hz/s]				
	Lim.	$C = 1$		$C = 2$		Lim.	$C = 1$		$C = 2$		Lim.	$C = 1$		$C = 2$	
		TKF	*W-TKF*	*TKF*	*W-TKF*		*TKF*	*W-TKF*	*TKF*	*W-TKF*		*TKF*	*W-TKF*	*TKF*	*W-TKF*
Freq. Dev. only (±2 Hz)	1	0.09	0.08	0.04	0.04	5	24	24	16	16	0.4	11.3	10.2	0.9	1.1
Freq. Dev (±2Hz) + 1% 2nd Harmonic	1	1.86	0.23	0.32	0.08	5	275	32	44	18	0.4	232	25.7	9.1	1.5
Freq. Dev (±2Hz) + 1% 3rd Harmonic	1	0.82	0.15	0.10	0.08	5	260	35	41	17	0.4	120	18.5	3.6	1.1
Freq. Dev (±2Hz) + 1% 50th Harmonic	1	0.20	0.10	0.05	0.04	5	47	22	18	17	0.4	24.2	9.3	1.1	1.0
AM (2 Hz 10% modulating tone)	3	0.09	0.11	0.04	0.09	60	17	15	4	5	2.3	10.5	10.3	0.6	0.8
PM (2 Hz 0.1 rad modulating tone)	3	0.09	0.11	0.04	0.08	60	14	30	4	48	2.3	9.5	10.8	0.7	1.3
Step Test (±10% amplitude change)	-	8.10	6.10	5.65	5.90	-	722	203	133	64	-	418	87.0	24.0	5.7
Step Test (±π/18 phase angle change)	-	14.60	10.50	9.82	10.30	-	2746	1381	1123	702	-	830	223	137	34.0
Linear freq. ramp (within ±2 Hz @±1 Hz/s)	1	0.09	0.10	0.04	0.06	10	17	18	14	28	0.4	10.0	11.0	0.8	1.0

The main remarks emerging from the results reported in both Tables can be summarized as follows.

- Disturbance whitening is maximally effective in the presence of harmonics (especially the low-order ones over one-cycle intervals). However, the relative impact of harmonics whitening decreases and becomes negligible for high-order harmonics regardless of which window function is used. The results obtained with the harmonics ranging from the 4th to the 49th are omitted in both Tables, since they are included between those related to the 3rd and the 50th harmonic.
- If just static off-nominal frequency deviations or slowly varying linear frequency changes affect the AC waveform, the influence of the whitening technique is generally negligible, as expected, since the fundamental component is preserved by linear transformation (6).
- When AM and PM modulations are considered, the effect of the whitening technique is almost negligible over one-cycle observation intervals. However, the estimation accuracy degradation grows worse over two-cycle intervals, which is in line with the results reported in [21]. This is probably due to the fact that by prolonging the observation intervals, a more accurate estimate of Q_r tends to whiten not only the disturbances, but also the modulating components in amplitude and phase, thus decreasing the TKF capability to track them effectively.
- In the tests with amplitude and phase step changes, the obtained results are globally very encouraging despite the whitening technique is not conceived to improve estimation accuracy under transient conditions. An impressive decrease of the maximum TVE and, above all, the maximum |FE| and |RFE| values can indeed be obtained with the W-TKF in almost all conditions, with the only exception of the TVE values computed over two-cycle observation intervals.

Overall, it is worth noticing that the W-TKF returns TVE values compliant with the *P Class* limits reported in the IEEE/IEC Standard even over one-cycle intervals, which is a remarkable achievement. The |FE| and |RFE| values instead, despite a major reduction, are generally still well beyond the IEEE/IEC Standard *P Class* limits. Nevertheless, a closer analysis of the Table reveals that in some cases (e.g., in the case of off-nominal frequency offsets) also the maximum |FE| and |RFE| values of the basic TKF heavily exceed the IEEE/IEC Standard limits. The fact that the |FE| and |RFE| values are comparable with those obtained with the W-TKF suggests that the current accuracy limitations in frequency and ROCOF estimation are mainly due to the sensitivity of the chosen Kalman filter to possible off-nominal frequency deviations and *not* to the whitening technique per se.

To evaluate more clearly the harmonics rejection capability of the W-TKF, the maximum TVE, |FE| and |RFE| values computed over 5 million one-cycle and two-cycle observation intervals (using the rectangular or the Hann window, respectively) are plotted in Fig. 1 as a function of the off-nominal frequency deviation in the range ±2 Hz, when all harmonics from the 2nd to the 25th affect the input waveform. The amplitude of all harmonics is set equal to 1% of the fundamental, so that the Total Harmonic Distortion (THD) is about 5% which is quite realistic. The SNR due to wideband noise only is again 64 dB. The sensitivity to the off-nominal frequency deviations on estimation accuracy is well visible in all cases. It is clear that in this case (with AM and PM oscillations the opposite result would be obtained), the results

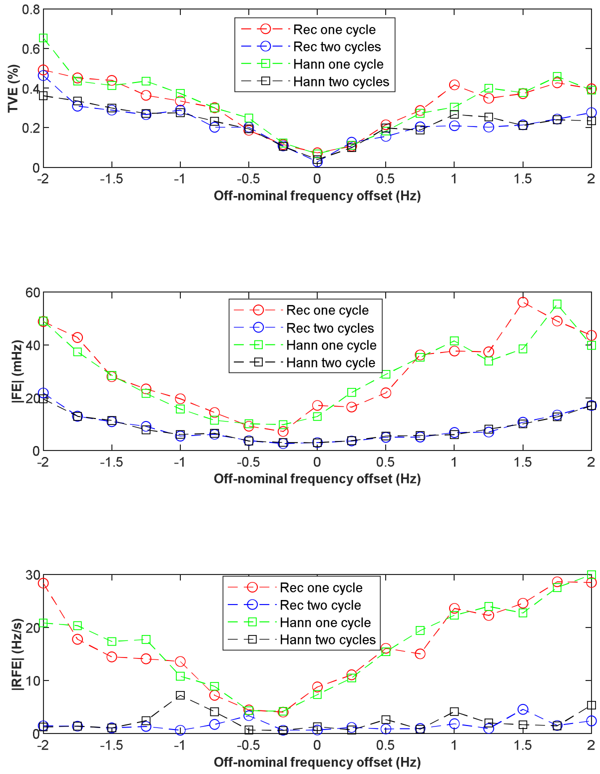

Fig. 1. Maximum TVE, |FE| and |RFE| values obtained with the W-TKF over one-cycle and two-cycle observation intervals (using the rectangular or the Hann window, respectively) when the harmonics from the 2nd to the 25th (each one with amplitude equal to 1% of the fundamental) affect the input AC waveform

over two cycles are better than those over one cycle, regardless of which window is used. Moreover, the difference between the |RFE| curves over two-cycle and one-cycle intervals is higher than the difference between the corresponding |FE| curves. This difference is in turn higher than the difference between the TVE curves over two-cycle and one-cycle intervals, respectively. This result is expected since synchrophasor, frequency and ROCOF, estimation exhibits an increasing nonlinear sensitivity to wideband noise [27], whose total power is further increased by the whitening technique.

IV. Conclusions

This paper presents a Whitening-based Taylor Kalman Filter (W-TKF) which improves the performance of a basic TKF for synchrophasor estimation through a preliminary decorrelation of the narrowband disturbances (e.g., harmonics) affecting AC voltage or current waveforms in power systems. The results obtained in most of the testing conditions specified in the IEEE/IEC Standard 60255-118-1-2018 show a remarkable accuracy improvement in steady-state conditions, although the effect of possible static off-nominal frequency deviations is not compensated. The proposed approach is maximally effective (especially over one-cycle intervals) in the presence of a significant total harmonic distortion, e.g., due to nonlinear loads. Also, it is particularly suitable for *P Class* PMUs that typically require higher responsiveness. In fact, quite unexpectedly, tangible benefits were observed even when amplitude or phase steps occur, e.g., due to possible faults. The TVE, |FE| and |RFE| values tend instead to be slightly worse when amplitude or phase modulations are considered. Despite the reported accuracy improvements, the full compliance with the requirements of the IEEE/IEC Standard at the moment cannot be reached because some |FE| and |RFE| exceed the prescribed limits. However, such performance limitations are due to the chosen Kalman filter and not to the whitening technique. The impact of the window function used to weigh the data collected in the update step of the filter is minor in the case considered.

REFERENCES

[1] M. M. Albu, M. Sănduleac, and C. Stănescu, "Syncretic Use of Smart Meters for Power Quality Monitoring in Emerging Networks," *IEEE Trans. Smart Grid*, vol. 8, no. 1, pp. 485–492, Jan. 2017, doi: 10.1109/TSG.2016.2598547.

[2] P. Castello, C. Laurano, C. Muscas, P. A. Pegoraro, S. Toscani, and M. Zanoni, "Harmonic Synchrophasors Measurement Algorithms with Embedded Compensation of Voltage Transformer Frequency Response," *IEEE Trans. Instrum. Meas.*, vol. 70, 2021, doi: 10.1109/TIM.2020.3042317.

[3] A. Bashian, M. Assili, and A. Anvari-Moghaddam, "A security-based observability method for optimal PMU-sensor placement in WAMS," *Int. J. Electr. Power Energy Syst.*, vol. 121, p. 106157, Oct. 2020, doi: 10.1016/j.ijepes.2020.106157.

[4] C. Lin, W. Wu, and Y. Guo, "Decentralized Robust State Estimation of Active Distribution Grids Incorporating Microgrids Based on PMU Measurements," *IEEE Trans. Smart Grid*, vol. 11, no. 1, pp. 810–820, Jan. 2020, doi: 10.1109/TSG.2019.2937162.

[5] R. Andreoni, D. Macii, M. Brunelli, and D. Petri, "Tri-Objective Optimal PMU Placement including Accurate State Estimation: The Case of Distribution Systems," *IEEE Access*, vol. 9, pp. 62102–62117, 2021, doi: 10.1109/ACCESS.2021.3074579.

[6] A. Bashian, M. Assili, and A. Anvari-Moghaddam, "Optimal Placement of PMUs and Related Sensor-based Communication Infrastructures for Full Observability of Distribution Networks," in *IEEE Power and Energy Society General Meeting*, Aug. 2020, vol. 2020-August, doi: 10.1109/PESGM41954.2020.9281586.

[7] D. Belega, D. Macii, and D. Petri, "Power system frequency estimation accuracy of improved DFT-based algorithms over short intervals," in *IEEE International Workshop on Applied Measurements for Power Systems, AMPS 2016 - Proceedings*, doi: 10.1109/AMPS.2016.7602810.

[8] "IEEE/IEC 60255-118-1-2018 - IEEE/IEC International Standard - Measuring relays and protection equipment - Part 118-1: Synchrophasor for power systems - Measurements, 2018" .

[9] G. Barchi, D. Fontanelli, D. Macii, and D. Petri, "On the accuracy of phasor angle measurements in power networks," *IEEE Trans. Instrum. Meas.*, vol. 64, no. 5, pp. 1129–1139, May 2015, doi: 10.1109/TIM.2014.2363752.

[10] K. Duda and T. P. Zielinski, "P Class and M Class Compliant PMU Based on Discrete-Time Frequency-Gain Transducer," *IEEE Trans. Power Deliv.*, pp. 1–1, 2021, doi: 10.1109/TPWRD.2021.3076831.

[11] D. Macii, D. Petri, and A. Zorat, "Accuracy analysis and enhancement of DFT-based synchrophasor estimators in off-nominal conditions," *IEEE Trans. Instrum. Meas.*, vol. 61, no. 10, pp. 2653–2664, 2012, doi: 10.1109/TIM.2012.2199197.

[12] B. Jafarpisheh, S. M. Madani, and S. Jafarpisheh, "Improved DFT-Based phasor estimation algorithm using down-sampling," *IEEE Trans. Power Deliv.*, vol. 33, no. 6, pp. 3242–3245, Dec. 2018, doi: 10.1109/TPWRD.2018.2831005.

[13] D. Macii, D. Belega, and D. Petri, "Ipdft-tuned estimation algorithms for pmus: Overview and performance comparison," *Appl. Sci.*, vol. 11, no. 5, pp. 1–22, Mar. 2021, doi: 10.3390/app11052318.

[14] M. A. Platas-Garza and J. A. De La O Serna, "Dynamic phasor and frequency estimates through maximally flat differentiators," *IEEE Trans. Instrum. Meas.*, vol. 59, no. 7, pp. 1803–1811, Jul. 2010, doi: 10.1109/TIM.2009.2030921.

[15] D. Belega, D. Fontanelli, and D. Petri, "Dynamic phasor and frequency measurements by an improved taylor weighted least squares algorithm," *IEEE Trans. Instrum. Meas.*, vol. 64, no. 8, pp. 2165–2178, Aug. 2015, doi: 10.1109/TIM.2014.2385171.

[16] P. Tosato, D. Macii, M. Luiso, D. Brunelli, D. Gallo, and C. Landi, "A Tuned Lightweight Estimation Algorithm for Low-Cost Phasor Measurement Units," *IEEE Trans. Instrum. Meas.*, vol. 67, no. 5, pp. 1047–1057, May 2018, doi: 10.1109/TIM.2017.2775458.

[17] M. A. Platas-Garza and J. A. De La O Serna, "Dynamic harmonic analysis through Taylor-Fourier transform," *IEEE Trans. Instrum. Meas.*, vol. 60, no. 3, pp. 804–813, Mar. 2011, doi: 10.1109/TIM.2010.2064690.

[18] D. Belega and D. Petri, "Fast procedures for accurate parameter estimation of sine-waves affected by noise and harmonic distortion," *Digit. Signal Process. A Rev. J.*, vol. 114, p. 103035, Jul. 2021, doi: 10.1016/j.dsp.2021.103035.

[19] M. Bertocco, G. Frigo, C. Narduzzi, C. Muscas, and P. A. Pegoraro, "Compressive Sensing of a Taylor-Fourier Multifrequency Model for Synchrophasor Estimation," *IEEE Trans. Instrum. Meas.*, vol. 64, no. 12, pp. 3274–3283, Dec. 2015, doi: 10.1109/TIM.2015.2450295.

[20] A. Derviskadic, P. Romano, and M. Paolone, "Iterative-Interpolated DFT for Synchrophasor Estimation: A Single Algorithm for P-and M-Class Compliant PMUs," *IEEE Trans. Instrum. Meas.*, vol. 67, no. 3, pp. 547–558, Mar. 2018, doi: 10.1109/TIM.2017.2779378.

[21] D. Macii, G. Barchi, and D. Fontanelli, "Decorrelation-based Harmonic Distortion Reduction for Synchrophasor Measurements," in *AMPS 2017 - IEEE International Workshop on Applied Measurements for Power Systems, Proceedings*, Sep 2017, doi: 10.1109/AMPS.2017.8078321.

[22] D. Fontanelli, D. Macii, and D. Petri, "Dynamic synchrophasor estimation using Smoothed Kalman filtering," in *IEEE Instrumentation and Measurement Technology Conference, May 2016,* doi: 10.1109/I2MTC.2016.7520462.

[23] J. A. De La O Serna and J. Rodríguez-Maldonado, "Instantaneous oscillating phasor estimates with TaylorK-Kalman filters," *IEEE Trans. Power Syst.*, vol. 26, no. 4, pp. 2336–2344, Nov. 2011, doi: 10.1109/TPWRS.2011.2157539.

[24] C. Muscas, P. A. Pegoraro, S. Sulis, M. Pau, F. Ponci, and A. Monti, "New Kalman Filter Approach Exploiting Frequency Knowledge for Accurate PMU-Based Power System State Estimation," *IEEE Trans. Instrum. Meas.*, vol. 69, no. 9, pp. 6713–6722, Sep. 2020, doi: 10.1109/TIM.2020.2977744.

[25] R. Ferrero, P. A. Pegoraro, and S. Toscani, "Dynamic Synchrophasor Estimation by Extended Kalman Filter," *IEEE Trans. Instrum. Meas.*, vol. 69, no. 7, pp. 4818–4826, Jul. 2020, doi: 10.1109/TIM.2019.2955797.

[26] Y. Bar-Shalom, X. Rong Li, *Estimation with Applications to Tracking and Navigation: Theory Algorithms and Software | Wiley*. Hoboken, NJ, USA: Wiley, 2001.

[27] D. Macii, D. Fontanelli, G. Barchi, and D. Petri, "Impact of Acquisition Wideband Noise on Synchrophasor Measurements: A Design Perspective," *IEEE Trans. Instrum. Meas.*, vol. 65, no. 10, pp. 2244–2253, Oct. 2016, doi: 10.1109/TIM.2016.2594023.